Cross-Validation of Scatterometer Measurements via Sea-Level Pressure Retrieval

Jérôme Patoux and Ralph C. Foster

***Abstract*—A combined analysis of ocean surface wind vector measurements by the European Advanced Scatterometer (ASCAT) and the National Aeronautics and Space Administration QuikSCAT (QS) scatterometer using buoy measurements, numerical weather prediction model analyses, and spectral decomposition reveals significant statistical differences between the two data sets. While QS wind speeds agree better with buoy wind speeds than ASCAT above 15 m s^{-1}, ASCAT wind directions agree better with buoy directions overall than QS. In contrast, it is shown that sea-level pressure (SLP) fields derived from ASCAT and QS measurements compare better with each other than the winds in a statistical sense, even though ASCAT bulk pressure gradients (BPGs) are slightly weaker than buoy pressure gradients and have slightly lower spectral energy than QS. Weaker BPGs in ASCAT are consistent with the low bias in ASCAT wind speeds. Thus, it is proposed that scatterometer-derived SLP fields can be used as a filter to improve the wind directions. This improves the QS wind directions but has less effect on the more accurate ASCAT wind directions. The unfiltered ASCAT wind vector statistics compare well with the statistics of the direction-filtered QS winds. It is suggested that this methodology might provide a basis for minimizing the discrepancies between various satellite wind measurement data sets in view of producing a long-term record of satellite-derived SLP fields and ocean surface wind vectors.**

***Index Terms*—Advaned Scatterometer (ASCAT), ocean surface winds, planetary boundary layer modeling, QuikSCAT, scatterometer, sea-level pressure, spaceborne radar, wind validation.**

I. Introduction

OCEAN vector winds measured by satellite have revolutionized our view of the oceanic surface wind field and our understanding of many atmospheric and oceanic processes [1], [2]. A relatively long-term satellite surface wind vector record began with the European Remote Sensing 1 (ERS-1) satellite in 1992 and has been continued to the present with ERS-2, the National Aeronautics and Space Administration scatterometers (NSCAT), SeaWinds-on-QuikSCAT (QS), and SeaWinds-on-ADEOS-II, the WindSat radiometer developed by the Naval Research Laboratory, and the ongoing European Advanced Scatterometer (ASCAT) mission. Although there is currently a nearly two-decade-long record of satellite ocean vector wind measurements, constructing a long-term climate record from multiple sensors and satellites presents a major challenge. There are significant technological differences between sensors, important algorithmic differences in wind retrieval, and large differences in spatial and temporal sampling. What might be interpreted as a trend in surface wind characteristics (or other derived geophysical quantity) could very well be a bias in the measurements or in the wind retrieval that was introduced by the transition from one instrument to another. We are reminded of these issues each time we have to face the demise of a satellite, as was recently the case with QS, and are forced to transition to other sources of measurements. To ensure a certain level of continuity, we need to cross-calibrate the old and new instruments. With the forthcoming availability of ocean vector wind measurements by multiple scatterometers in space, such as the ongoing ASCAT mission and OSCAT on Oceansat-2 from the Indian Space Research Organization (ISRO), as well as the future scatterometers on HY-2A and HY-2B from the China National Space Administration, GCOM-W2 launched by the Japanese Aerospace Exploration Agency, METOP B (ESA), Oceansat-3 (ISRO), and on the Meteor satellite series proposed by the Russian Federal Space Agency, the need for cross-validation techniques becomes even more pressing.

Scatterometer winds are traditionally calibrated and validated using numerical weather prediction (NWP) model analyses and buoy measurements [3]–[7]. They are further cross-validated with other instruments using statistical comparisons of wind vector components, direction, and speed [8]–[10]. Here, we propose an additional methodology for cross-validating scatterometer measurements by comparing statistical characteristics of sea-level pressure (SLP) fields derived from the wind measurements using a planetary boundary layer (PBL) model [11]. It provides an alternative method that is complementary to existing statistical techniques. It has the advantage of comparing quantities at the scale of the satellite swath, which for QS approaches the synoptic scale, rather than at the scale of the wind vector cell. Additionally, these SLP fields can be used to derive a new set of ocean surface wind vectors with, in the case of QS for example, improved statistical characteristics [12]. These new wind vectors can also be used for validation purposes.

We will illustrate the proposed methodology by comparing ASCAT-derived SLP fields and winds with QS-derived products. The data are presented in Section II, while Section III contains a preliminary exploration of the statistical differences between the two sets of wind vectors. Section IV contains

Manuscript received May 21, 2011; revised August 29, 2011; accepted October 1, 2011. Date of publication December 2, 2011; date of current version June 20, 2012. The National Center for Atmospheric Research is supported by grants from the National Science Foundation. The authors acknowledge NASA OVWST grant support under JPL subcontract 1285663 and NASA Grant NNX10AO87G.

J. Patoux is with the Department of Atmospheric Sciences, University of Washington, Seattle, WA 98195-1640 USA (e-mail: jerome@atmos.washington.edu).

R. C. Foster is with the Applied Physics Laboratory, University of Washington, Seattle, WA 98105-6698 USA (e-mail: ralph@apl.washington.edu).

Color versions of one or more of the figures in this paper are available online at http://ieeexplore.ieee.org.

Digital Object Identifier 10.1109/TGRS.2011.2172620

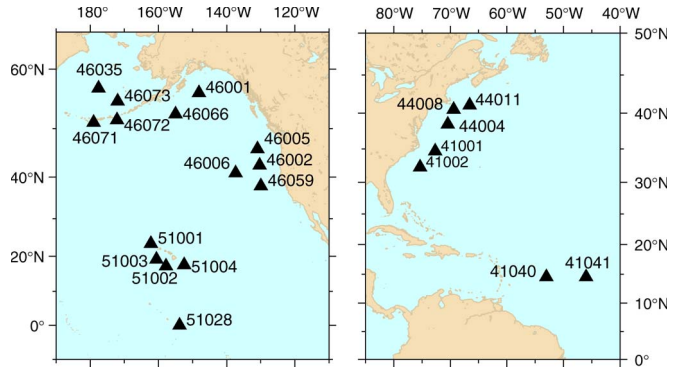

Fig. 1. Locations of the NDBC buoys used in the correlation calculations.

the SLP field comparisons. In Section V, the wind filtering via SLP retrieval is discussed, and the filtered wind products are compared. Although the methodology is illustrated with ASCAT and QS winds, it is applicable to any set of satellite wind measurements, as will be discussed in Section VI.

II. Scatterometers, Buoys, and Model Analyses

We used 10 years (2000–2009) of the standard L2B swath-based QS surface wind vectors distributed by the Jet Propulsion Laboratory Physical Oceanography Distributed Active Archive Center, with 25-km resolution. Areas contaminated by rain were identified using the provided MUDH rain flag [13]. For comparison, we also used the QS winds filtered with the Direction Interval Retrieval with THresholded nudging (DIRTH) algorithm [14].

In parallel, we used 34 months (from March 2007 to November 2009) of Level 2 ASCAT surface wind vectors distributed by the EUMETSAT Ocean and Sea Ice Satellite Application Facility (OSI SAF), with a 25-km sampling resolution and a 50-km effective resolution. We added 0.2 m s^{-1} to the winds prior to 20 November 2008 to convert them from real to neutral-equivalent 10-m winds, as recommended by the OSI SAF.

Buoy surface wind measurements were obtained from the NOAA National Data Buoy Center (NDBC) in the form of hourly reports. They have a precision of 1° and an accuracy of 10° in direction, a precision of 0.1 m s^{-1}, and an accuracy of 1 m s^{-1} or 10% (whichever is greater) in wind speed. The surface pressure measurements have a precision of 0.1 hPa and an accuracy of 1 hPa. The sea-surface and air temperature measurements have a precision of 0.1 °C and an accuracy of 1 °C (see NDBC homepage http://ndbc.noaa.gov/rsa.shtml). For buoy comparisons in which the wind was measured at 5-m height, a neutral-equivalent wind vector was calculated at 10 m (see below). The buoys used in this study are shown in Fig. 1.

The model SLP fields were extracted from the ds111.1 European Centre for Medium-Range Weather Forecasts (ECMWF) surface analyses obtained from the National Center for Atmospheric Research (NCAR). These analyses are output on a Gaussian $(n80)$ grid with a resolution of about 1.125°. They were interpolated to the location and time of the scatterometer wind vectors by trilinear interpolation. Note that ECMWF started assimilating QS winds on 22 January 2002 and ASCAT winds on 12 June 2007.

III. Preliminary Wind Vector Comparison

The statistical differences between the two scatterometer wind data sets are first explored in three ways: 1) with a linear regression of the differences with buoy wind measurements, 2) a root mean square (rms) comparison with ECMWF surface wind analyses, and 3) a spectral analysis of the horizontal structure of the wind fields.

A. Comparison With Buoy Measurements

We start by comparing ASCAT and QS wind measurements with NDBC buoy measurements. As noted by [12], care must be taken when interpreting the results of a statistical analysis of the difference between buoy and scatterometer winds, as they measure fundamentally different quantities (temporal mean at a fixed location versus instantaneous spatial average relative to a moving sea surface) and are neither perfectly temporally nor spatially colocated, which can induce large errors in the presence of small-scale transients. Following [5] and [12], we therefore only considered buoy measurements that occurred within 50 km and 30 min of a QS or ASCAT wind vector. Since QS and ASCAT winds are 10-m neutral equivalent, we first converted the buoy winds to neutral-equivalent winds at 10-m height. We used the roughness length parametrizations and stratification corrections of the 2003 updates to the Coupled Ocean-Atmosphere Response Experiment parametrization [15], [16], along with the air temperature, sea-surface temperature, and dew point temperature measured by the buoy.

The two wind products are compared in Figs. 2 and 3 in rain-free conditions. QS DIRTH wind statistics are also shown for reference. (The dashed lines for QS/SLP_u10 and AS/SLP_u10 will be discussed in Section V.) Fig. 2(a) shows that, above 5 m s^{-1}, ASCAT wind speeds tend to be lower than the corresponding buoy wind speeds with a difference that increases with increasing wind speed. While QS wind speeds follow a similar behavior at low wind speeds, they are in better agreement with the buoys above 15 m s^{-1}.

Fig. 2(b) shows that ASCAT wind directions, in contrast, are in better agreement with the buoy measurements than QS wind directions. Directional errors in the retrieval of QS winds are well documented, in particular at nadir and on the edges of the swath [10], [17]. QS uses two conically scanning antenna beams at different incidence angles. Where the ocean is observed at four distinct look angles, the quality of the wind retrieval is improved (the so-called "sweet spots"). In the outer edges of the swath, where only one beam is making observations, and at nadir, where the four measurements are made at 0° or 180° azimuth, the quality of the wind retrieval is degraded. Although not shown here, the QS rms errors observed in Fig. 2(b) are indeed larger at nadir (wind vector cells 27–50) and on the edges (wind vector cells 3–14 and 63–74) than in the sweet spots (wind vector cells 15–26 and 51–62).

These results are confirmed by the analysis of the zonal and meridional wind components in Fig. 3 and the corresponding regression coefficients summarized in Table I. The R^2 correlation coefficients for ASCAT are 0.94 (for u) and 0.91 (for v), which is higher than the correlation coefficient obtained with any of the other products. The slope of the lines of

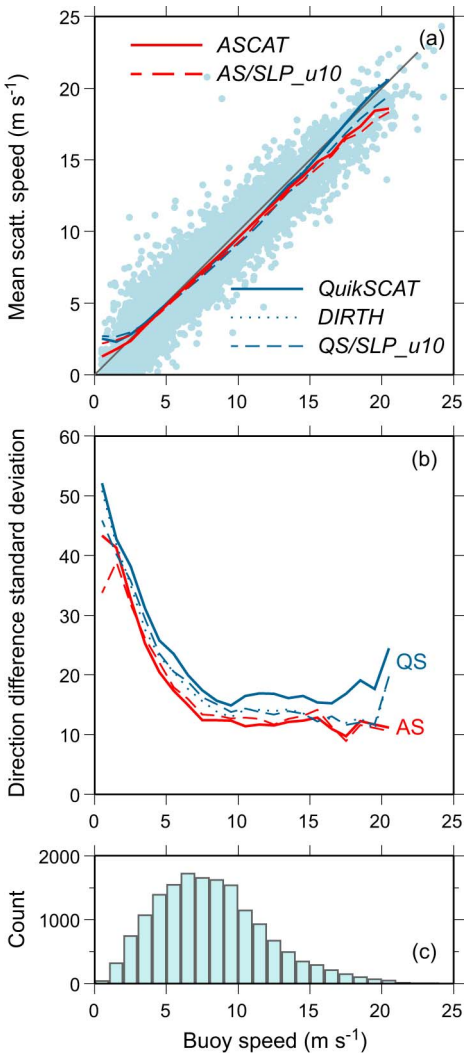

Fig. 2. Comparison of ASCAT, QS, and DIRTH winds with buoy wind measurements. (a) Conditional mean wind speeds as a function of buoy wind speed. The blue cloud of points in the background is representative of ASCAT-buoy pairs for illustration. Since DIRTH filters mostly for direction, the DIRTH wind speeds are almost identical to the original QS wind speeds, and the dotted line is almost coincident with the solid blue line. (b) Standard deviation of wind direction differences as a function of buoy wind speed. (c) Frequency distribution of buoy wind speeds.

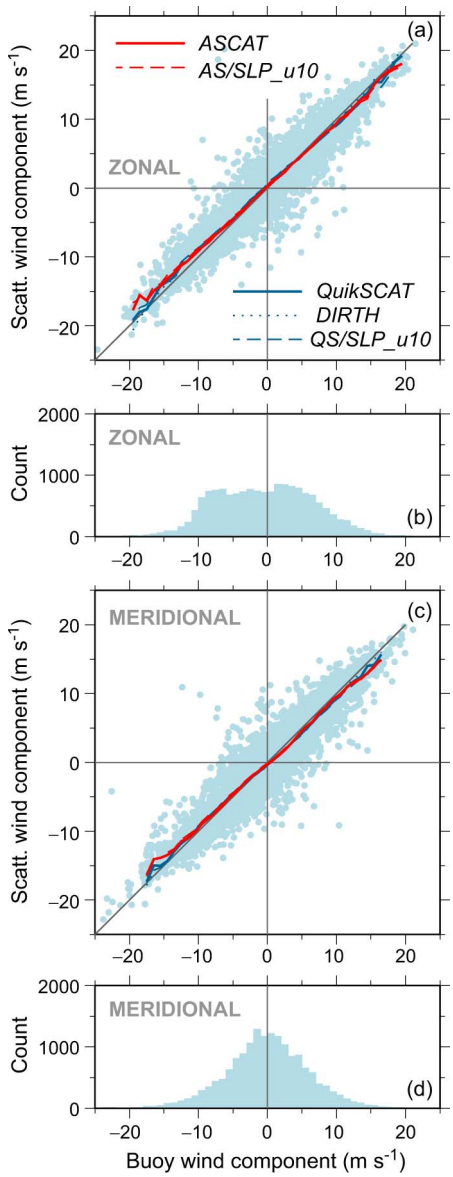

Fig. 3. Comparison of ASCAT, QS, and DIRTH winds with buoy wind measurements. (a) Conditional mean zonal component as a function of buoy wind component. (c) Conditional mean meridional component as a function of buoy wind component. The blue clouds of points in the background are representative of ASCAT-buoy pairs for illustration. (b), (d) Frequency distribution of buoy wind components.

regression, however, is 0.93 for both wind components, which confirms that the discrepancy between ASCAT winds and buoy measurements is due to low values of wind speed more than directional errors. This is confirmed by a principal component analysis, in which the slope of the first principal component is less for ASCAT than it is for QS or DIRTH.

We should mention that the standard deviation of the directional differences between QS and buoy measurements does not appear to be constant over the full 1999–2009 period. Fig. 4 compares the standard deviation for the period 2004–2006 to the period 2007–2009. There appears to be a significant difference between about 10 and 15 m s^{-1}, with a degradation of the agreement between QS and buoys toward the later years of QS. This difference persists when various subsets of buoys are used in the comparison, as well as when the 2007–2009 period is compared to the full 1999–2006 period. It is not clear at this point if this difference is due to a change in the quality of the buoy measurements or to a degradation of the quality of the QS wind retrieval. It could, for example, be due to a reduced sampling of the ocean surface (in particular, a reduced range of azimuthal "looks") due to the slowing antenna rotation observed toward the end of the life of QS and needs to be investigated further.

Overall, to summarize, this first analysis suggests that ASCAT wind directions are more accurate than QS wind directions, but QS wind speeds are more accurate than ASCAT wind speeds, when compared to buoy measurements.

B. Comparison With ECMWF Surface Winds

The scatterometer winds are now compared to NWP model surface wind analyses over the Pacific Ocean by calculating,

TABLE I
REGRESSION OF ASCAT, AS/SLP_u10, QS, DIRTH, AND QS/SLP_u10 AGAINST BUOY WIND COMPONENTS: REGRESSION COEFFICIENT R^2, y-INTERCEPT a, SLOPE b, AND SLOPE OF THE FIRST PRINCIPAL COMPONENT SPC

	ASCAT	AS/SLP_u10	QS	DIRTH	QS/SLP_u10
			Zonal component (u)		
R^2	0.94	0.93	0.89	0.92	0.91
a	0.15±0.03	0.32±0.03	0.26±0.03	0.30±0.03	0.35±0.03
b	0.93±0.00	0.91±0.00	0.93±0.01	0.95±0.00	0.90±0.00
SPC	0.96	0.94	0.99	0.99	0.94
			Meridional component (v)		
R^2	0.91	0.90	0.85	0.87	0.86
a	-0.14±0.03	-0.01±0.03	-0.18±0.03	-0.19±0.03	-0.17±0.03
b	0.93±0.00	0.91±0.00	0.90±0.01	0.92±0.01	0.89±0.01
SPC	0.97	0.95	0.98	0.98	0.96

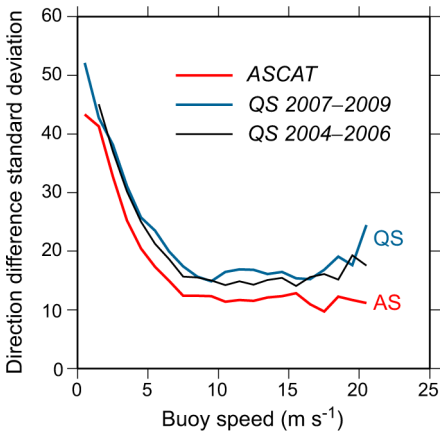

Fig. 4. Comparison of the standard deviation of wind direction differences between QS and buoy winds as a function of buoy wind speed, for the periods 2004–2006 and 2007–2009.

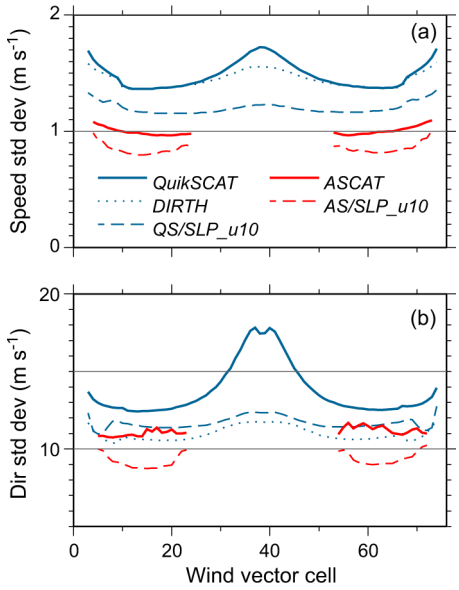

Fig. 5. Comparison of ASCAT, QS, DIRTH, and SLP_u10 winds with ECMWF analyses. (a) Speed standard deviation as a function of wind vector cell. (b) Wind direction standard deviation as a function of wind vector cell. QS wind vector cells are numbered from 1 to 76, with nadir between cells 38 and 39, while ASCAT wind vector cells are plotted according to their cross-track distance from nadir to match the QS wind vector cells.

for each swath, the standard deviation in speed and direction of the scatterometer winds with respect to ECMWF10-m winds. Following [10] and [12], we first interpolated the ECMWF 10-m winds to the geographic location and time of the scatterometer winds by trilinear interpolation, we removed cases where the scatterometer and interpolated ECMWF wind directions differed by more than 90°, and we averaged the results over the entire QS and ASCAT periods and along each individual swath as a function of wind vector cell to obtain Fig. 5.

The RMS differences between QS and ECMWF are on the order of 1.4–1.7 m s^{-1} in wind speed and 13°–18° in direction, while ASCAT winds are in better agreement with ECMWF winds, with differences on the order of 0.9–1.1 m s^{-1} in wind speed and 11°–12° in direction. Both panels show that the differences between QS and ECMWF wind vectors are largest at nadir and in the outer edges of the swaths, for the reasons described above. The cross-swath variations of the ASCAT measurements (corresponding roughly to QS sweet spots) are relatively small.

To better characterize the differences between the two instruments, we also perform separate analyses for the Northern (20° N–60° N) and Southern (60° S–20° S) Pacific Ocean, as well as for the Tropics. We average the standard deviations across the swath (i.e., over all wind vector cells), and we plot them as a function of time from 1999 to 2009 (Fig. 6).

The speed and directional differences can now be seen to exhibit seasonal variations of large, intermediate, and small amplitude in the Northern, Southern, and tropical Pacific Ocean, respectively. Patoux *et al.* [12] assigned the larger winter differences to the enhanced strength of the synoptic weather systems in that season. They assigned the larger seasonal variations in the northern hemisphere to the enhanced zonal temperature gradients and baroclinicity encountered in the Northern Pacific Ocean. They further noted the decrease in standard deviation after January 22, 2002, when ECMWF began assimilating QS winds.

It is interesting to note that, in spite of significant differences in the *magnitude* of the standard deviations, both ASCAT and QS exhibit similar temporal *variations* of the standard deviations. This confirms that there are differences in the retrieval of

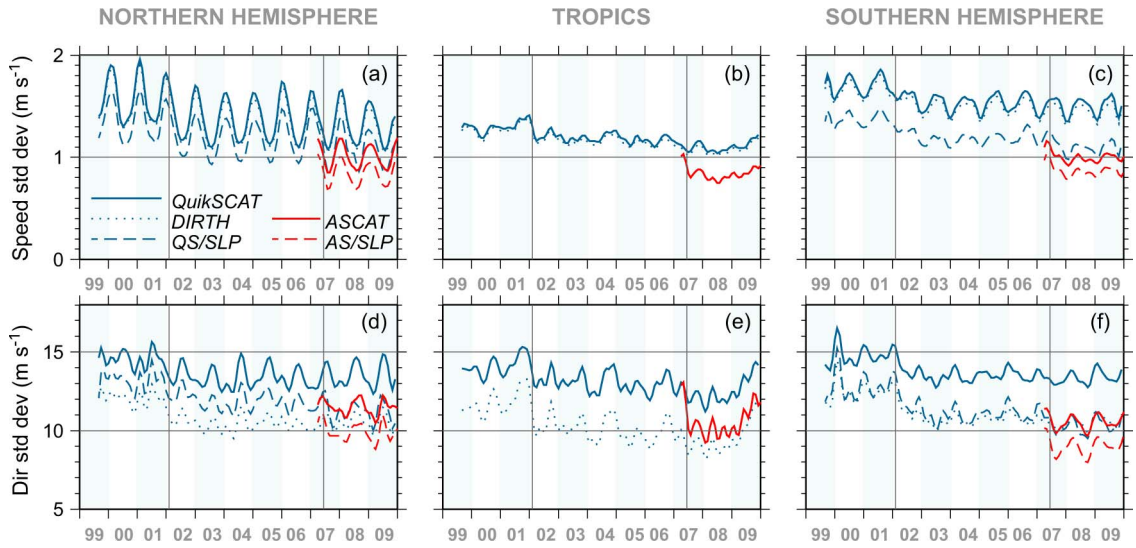

Fig. 6. Comparison of ASCAT, QS, DIRTH, and SLP_u10 winds with ECMWF analyses in the Northern Hemisphere (left), tropics (center), and Southern Hemisphere (right). (a), (b), (c) Speed standard deviation as a function of time (monthly averages). (d), (e), (f) Wind direction standard deviation as a function of time (monthly averages). The vertical gray lines show the start of QS and ASCAT assimilation by ECMWF on 22 January 2002 and 12 June 2007, respectively.

the wind direction and speed by ASCAT and QS, and that the two instruments are relatively similar in their ability to capture the overall large-scale structure of the wind field.

C. Spectral Analysis

We conclude our wind validation analysis with a spectral analysis of QS and ASCAT winds in the North Pacific Ocean. Following [18] and [19], we compute the power spectral density in the along-track direction and assume that the effects due to the spherical shape of the earth are negligible. The 25-km spacing translates into a wavenumber resolution of 0.000625 km^{-1} (1600 km) to 0.02 km^{-1} (50 km). We calculate along-track wavenumber spectra of the total wind for QS and ASCAT, as well as for the trilinearly interpolated ECMWF 10-m winds for comparison. We only keep the continuous lines of wind vectors and apply an end-point detrending. We concentrate on the North Pacific Ocean (20° N–50° N) in year 2008 for evaluation purposes, keeping in mind that the results will be slightly different in other ocean basins and at different times. The results were obtained from averaging 1104 QS swaths and 1435 ASCAT swaths. As a fair test to QS, the QS spectra were averaged over the sections of the swath where the wind retrieval is optimal (the so-called "sweet spots," wind vector cells 15–26 and 51–62) (Fig. 7). The confidence intervals are too small to be visible. They were estimated both from the confidence intervals of the log10 of the sample coefficients and as the standard deviation of the distribution of means obtained with a bootstrap method. The ratio of the error to the coefficient is on the order of 1% to 3%, increasing toward the smaller scales.

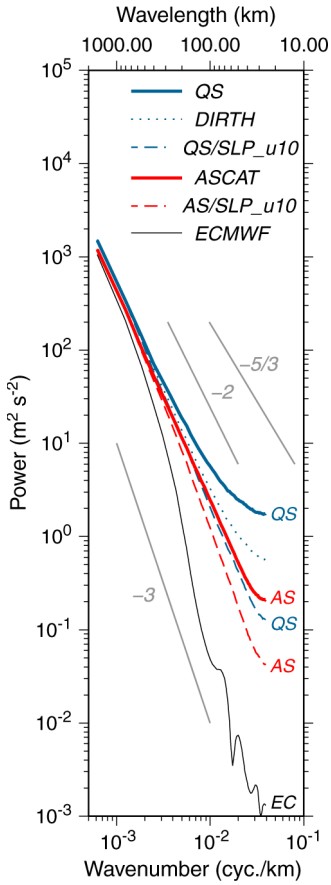

Fig. 7. Comparison of QS, DIRTH, SLP_u10, and ECMWF wind energy spectra.

As documented in [12], the QS power spectrum follows an approximate power law with a slope close to −2.0 down to 400–500 km, but departs from that behavior with increased variance at smaller scales. While DIRTH removes some of that small-scale energy, it still departs from a power law below 100–200 km. It has been proposed that this wavenumber range might correspond to a transition from an inverse cascade of energy of slope −5/3 (small-scale 3-D turbulence) to a downward cascade of energy of slope −3 (larger-scale 2-D geostrophic turbulence). The observed QS spectra, however, do not match the expected spectral slopes. The flattening of the spectra is more likely due to a white-noise saturation

associated with instrumental errors. These errors are due to errors associated with the instrument and errors associated with the model function and the wind retrieval. Rodriguez and Chau [20] demonstrated that this small-scale energy can be traced back to "shot-noise" created by isolated errors in the wind directions. The fact that the ASCAT spectrum follows a -2.2 power law down to very small scales suggests that the ASCAT measurements are not contaminated by such "shot-noise," in agreement with our previous results showing that ASCAT winds contain fewer directional errors than QS.

The ECMWF spectrum, in contrast, "falls off" rapidly below 1000 km and contains much less small-scale energy than any other wind product presented here. This fall-off, however, has been documented and can be attributed to the 1.125° resolution of the NWP model [18], [19], [21]–[25]. (Note that the structure at high wavenumber below 200 km is an artifact of the trilinear interpolation of the ECMWF winds to the QS observation locations [21].)

In summary, the ASCAT and QS wind data sets present significant statistical differences in both speed and direction, as well as in spectral characteristics. We are now interested in investigating whether these differences carry over to the pressure fields calculated from the wind measurements.

IV. Sea-Level Pressure Field Comparisons

Patoux *et al.* [11] used the University of Washington (UW) PBL model to compute swaths of SLP from QS wind measurements (referred to as QS/UWPBL surface pressure fields). They established that the rms difference between these QS/UWPBL surface pressure fields (when including a correction for stratification) and the closest-in-time ECMWF surface pressure analyses is only on the order of 2 hPa in the midlatitudes and 1 hPa in the tropics. They also compared the QS/UWPBL pressure fields with pairs of buoy pressure measurements and found a very good correlation of 0.968 between bulk pressure gradients (BPGs). Patoux *et al.* [26] confirmed the value of these scatterometer-derived SLP fields by showing that they contain mesoscale information that is absent from NWP analyses. In view of the demise of QS, it is thus of interest to determine whether similar SLP fields can be computed from ASCAT measurements, how they compare to QS-derived SLP fields, and whether the SLP retrieval can be used as a cross-validation tool. We now address these issues, after briefly describing the SLP retrieval methodology.

A. Methodology

For each scatterometer swath, a SLP field is calculated from the vector wind measurements using the UWPBL model described in [27] and the pressure retrieval method described in [28] and [29]. The resulting satellite-based SLP fields are archived and available at http://pbl.atmos.washington.edu for both QS and ASCAT. The pressure retrieval method has been extensively described in previous articles [11] and is only shortly summarized here.

A swath of gradient wind vectors is calculated from the surface wind vectors using the UWPBL model in its so-called "inverse" mode. The gradient wind vectors are translated into pressure gradients using the gradient wind correction described in [30]. A pressure field is fit to the swath of pressure gradients by least-squares minimization [28], [31] and slightly smoothed with a low-pass filter [32]. The analysis is repeated here for ASCAT over the 2007–2009 period.

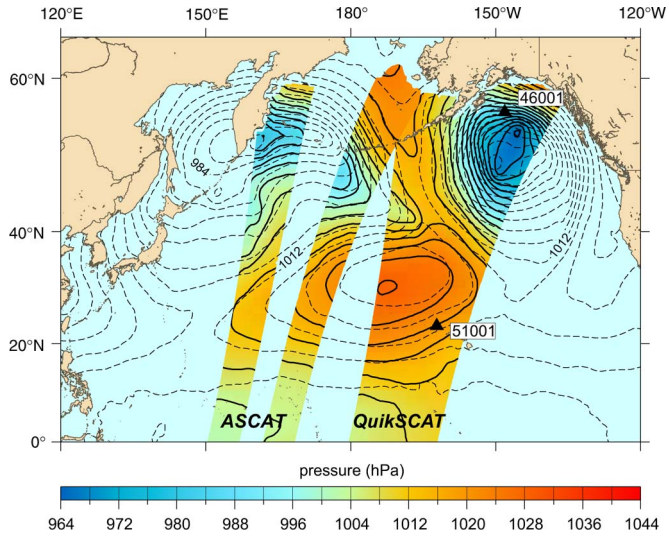

Fig. 8. Comparison of ASCAT- and QS-derived sea-level pressure fields (colors and solid isobars) on 31 December 2007 at 22:52 UTC (ASCAT dual swath on the left) and 1 January 2008 at 05:29 UTC (QS single broader swath on the right). The ECMWF sea-level pressure analysis on 1 January 2008 at 00:00 UTC is shown with dashed 4-hPa isobars for reference. Black triangles represent NDBC buoys.

An example of each type of swath is shown in Fig. 8. Note that QS had a rotating, conically scanning antenna that sampled the full range of azimuthal angles during each revolution, yielding a unique 1600-km wide swath of wind vector retrievals, with the highest accuracy in the sweet spots described above. ASCAT, in contrast, has two sets of antennas sampling two separate swaths of 550 km width, separated by about 700 km, as shown by the two independent SLP bands in Fig. 8. Ideally, we would want to compare QS/UWPBL pressure fields directly with ASCAT/UWPBL pressure fields. Due to the difference in the longitude of their ascending nodes, however, it is difficult to do so without introducing large temporal biases. Moreover, due to the smaller width of the ASCAT swaths, it is difficult to obtain sufficiently large intersections of swaths that useful pressure differences can be calculated. Therefore, in the present analysis, we choose to compare each product to a third estimate of pressure, i.e., buoy measurements in Section IV-B and NWP analyses in Section IV-C.

B. Comparison With Buoy Measurements

ASCAT- and QS-derived SLP fields are first compared to measurements of surface pressure by NDBC buoys. In following with [11], and because we are interested in comparing the pressure gradient structure of the UWPBL fields, we identify scatterometer swaths that pass over *two* buoys, as shown in Fig. 8 for buoys 46 001 and 51 001 in the case of QS. We calculate the pressure difference between the two buoys, which can be thought of as a BPG. We then compare the buoy BPG with the corresponding BPG in the UWPBL swath. We repeat

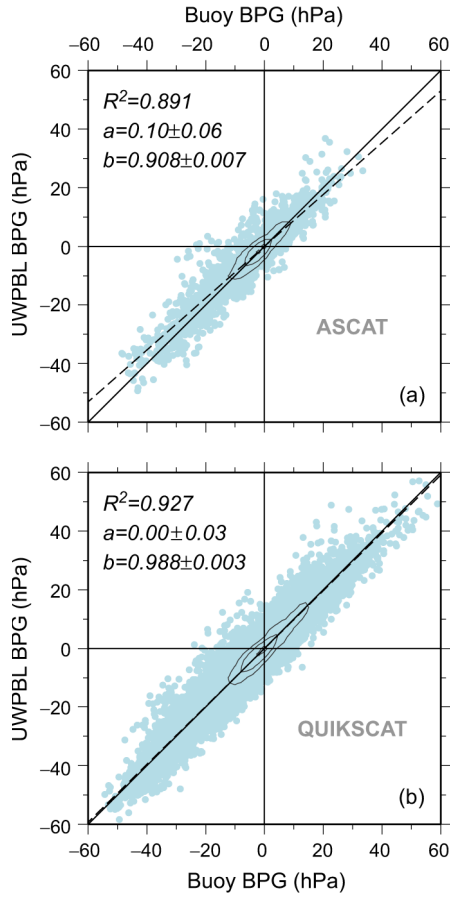

Fig. 9. Comparison of buoy and scatterometer-derived BPG. (a) ASCAT. (b) QuikSCAT.

this comparison for all QS and ASCAT swaths that cover these two buoys, and then for all possible pairs of buoys in the North Pacific and North Atlantic Oceans, as shown in Fig. 1. The results are summarized in Fig. 9 and show that the correlation coefficient between the ASCAT BPGs and the buoy BPGs ($R^2 = 0.891$) is lower than between the QS BPGs and the buoy BPGs ($R^2 = 0.927$). Maybe more importantly, the slope for ASCAT ($b = 0.908 \pm 0.007$) is less than the slope for QS ($b = 0.988 \pm 0.003$), which shows that the ASCAT BPGs tend to be weaker than the QS BPGs. Since the BPGs are a direct function of the strength of the winds, this is consistent with the first part of our analysis, where we showed that ASCAT wind speeds are overall lower than QS wind speeds (Section III).

C. Comparison With ECMWF Pressure Analyses

The UWPBL surface pressure fields are next compared with ECMWF surface pressure analyses by calculating the rms difference between each UWPBL swath and the corresponding ECMWF analysis, interpolated linearly to the time of the swath. An example of such a reference ECMWF SLP analysis is shown with dashed lines in Fig. 8. Since the mean difference between each UWPBL pressure field and the corresponding ECMWF analysis is forced to be zero, we are capturing differences in structure rather than differences in absolute values of pressure. Large rms differences will reflect discrepancies in both the magnitude and the location of synoptic features. Note, however,

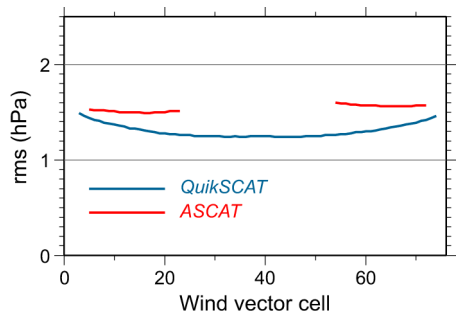

Fig. 10. Across-swath variations of the mean rms difference between ECMWF and scatterometer-derived pressure fields averaged over the ASCAT period.

that the ECMWF analyses contain their own errors in relation to the "truth." ECMWF analyses are known to be defective, for example, in areas of strong PBL stratification and baroclinicity, such as the vicinity of the Gulf Stream or the Aghulas Return Current, or areas of fetch and wind shadow effects near islands and coastlines, or due to the misplacement of atmospheric features such as low pressure centers or the InterTropical Convergence Zone (ITCZ) [10], [33], [34]. Thus, these comparisons do not inform us about the absolute errors of the UWPBL fields; the ECMWF analyses are used as a baseline, a "best estimate" of the SLP field against which the two scatterometer products are compared.

Fig. 10 shows that the overall rms difference between the QS/UWPBL SLP fields and the corresponding ECMWF analyses is 1.2–1.5 hPa, with a tendency for better agreement at the center of the swath. Note that the differences are relatively uniform across the swath, in contrast with the large cross-swath variations in wind speed and wind direction rms differences observed in Fig. 5. This flattening of the rms differences suggests that the SLP retrieval optimizes the SLP pattern to the swath as a whole, which makes it relatively insensitive to localized errors in the wind vectors, particularly to localized direction errors. Working inwards from the sweet spots improves the SLP in the nadir region. However, edge effects and higher errors in the swath edge vectors (Fig. 5) increase the SLP rms at the swath edges.

The rms difference between the AS/UWPBL and the corresponding ECMWF analyses is 1.5–1.6 hPa, or slightly larger than for QS. This global averaging, however, does not reflect seasonal and geographical differences between the two instruments. Therefore, we compute separate rms statistics for the northern (20° N–60° N) and southern (60° S–20° S) Pacific Ocean, as well as for the tropics (20° S–20° N). We further average the results to create a monthly time series of rms differences, as shown in Fig. 11. When so averaged, the QS/UWPBL differences exhibit an annual cycle around a mean of 1.7 hPa in the northern Pacific Ocean, 1.9 hPa in the southern Pacific Ocean, and 1.1 hPa in the tropics. Note that the seasonal variations are similar to those observed earlier in the wind differences (Fig. 6). There is better agreement with ECMWF analyses in summer than in winter, in the tropics than in the midlatitudes, and in the northern midlatitudes than in the southern midlatitudes. [11] assigned the smaller differences observed in the tropics and in the summer to the fact that the

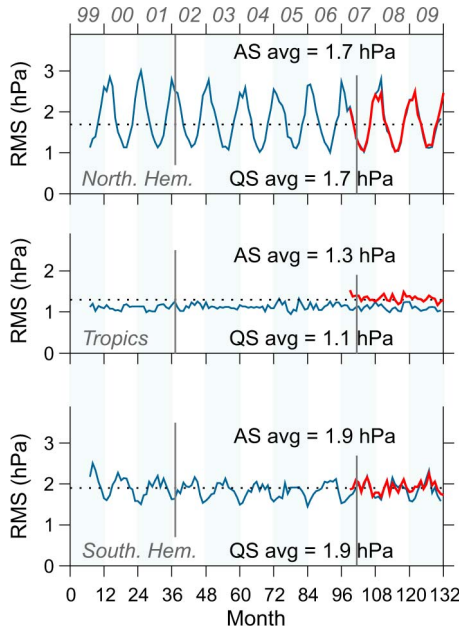

Fig. 11. Temporal variations of the monthly mean rms difference between ECMWF and scatterometer-derived pressure fields. Shown are ASCAT (red lines) and QS (blue lines) statistics for the Northern Hemisphere (top), Tropics (middle), and Southern Hemisphere (bottom). The dotted line shows the ASCAT mean. Averages are calculated over the ASCAT period. The vertical gray lines show the start of QS and ASCAT assimilation by ECMWF on 22 January 2002 and 12 June 2007, respectively.

pressure fields themselves comprise a narrower range of values in the tropics compared to the midlatitudes and in the summer midlatitudes compared to the winter midlatitudes. They also noted the better agreement between ECMWF and QS/UWPBL pressure fields with the assimilation of the QS measurements in the ECMWF NWP model starting on 22 January 2002.

The ASCAT/UWPBL differences are virtually identical to QS in the midlatitudes. In the tropics, the ASCAT differences are consistently 0.1–0.2 hPa larger than with QS. However, the UWPBL model is less accurate in the tropics compared to its performance in the midlatitudes [29]. It is not clear whether this discrepancy is due to a difference between the two instruments or to a limitation of the PBL model itself. Thus, in spite of small differences, Fig. 11 shows that the agreement between the two SLP data sets (with respect to ECMWF) is quite remarkable.

D. Spectral Analysis

The comparison of QS/UWPBL and ASCAT/UWPBL pressure fields is now complemented by an analysis of their spectral components. Fig. 12 shows average spectra computed from both QS/UWPBL and ASCAT/UWPBL pressure swaths over the Northern Pacific Ocean in 2008 (25° N to 45° N). We verified the consistency of the results by restricting the decomposition to ascending and descending swaths and performing separate decompositions on left and right ASCAT swaths (not shown). The spectra are also compared to the corresponding average ECMWF spectrum for that same period, calculated from the ECMWF SLP analyses interpolated in time and space to the ASCAT swaths.

In contrast with the wind spectra (Fig. 7), the three pressure spectra are strikingly similar, with only slightly more energy at

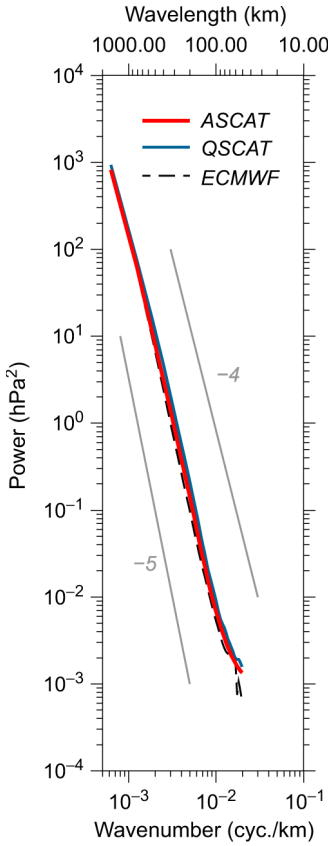

Fig. 12. Comparison of ASCAT, QS, and ECMWF pressure energy spectra.

all scales in the QS/UWPBL product as compared to ASCAT/UWPBL, and more energy in both scatterometer-derived products as compared to ECMWF. The slope of the spectra, as calculated by linear regression over the 100–1600 km wavelength range, is −4.3 for ASCAT and QS, and −4.4 for ECMWF.

The differences in spectral energy between ASCAT and QS are consistent with the differences observed in the magnitude of the BPGs in Section IV-B: overall weaker ASCAT BPGs should translate into weaker spectral components. The differences between the scatterometers and ECMWF suggest that the scatterometers capture more of the meso- to synoptic scale variability at wavelengths below 600–800 km, which is consistent with the results of [26].

The −4.3 slope of the scatterometer-derived pressure spectra suggests that the scatterometer wind spectra should have a slope of about −2.3 (see Appendix), i.e., slightly steeper than the −2.0 and −2.2 slopes found in Section III. This discrepancy can be explained by the fact that the pressure retrieval essentially acts as a low-pass filter. The individual wind vectors in a scatterometer swath are more or less independently derived. The SLP retrieval, however, considers the entire swath and seeks an optimal swath-wide solution, which, as we have shown, is generally quite accurate. We thus hypothesize that the SLP filtering has the strongest effect on the small-scale energy that is associated with instrumental noise. This results in a steeper SLP spectrum. This invites us to rederive a new set of reduced-noise winds from the pressure fields and to expect steeper wind energy spectra as well. Moreover, since the ASCAT/UWPBL and QS/UWPBL pressure fields are quite

similar in a statistical sense, it also invites us to investigate the extent to which the derived SLP fields can help us reconcile the wind measurements.

V. Wind Filtering via SLP Retrieval

Patoux *et al.* [12] showed that, when a new set of winds is derived from the QS/UWPBL pressure fields, now using the UWPBL model in its so-called "direct" mode, the new winds (hereafter, SLP_u10 winds) are in better agreement with buoy measurements and ECMWF analyses than the original QS winds, particularly in direction and in rainy conditions. (Note that this "direct" methodology is only currently available in the midlatitudes.) They claim that the information contained in the synoptic structure of the pressure field is effective at correcting errors at the scale of individual wind vector cells. They propose that the new winds could be used to 1) inform the ambiguity selection in the QS wind retrieval; 2) correct the direction of QS wind vectors, in all cases or above a certain threshold; or 3) replace the original QS winds altogether. Since the QS-derived and ASCAT-derived SLP fields are in remarkable agreement, it is legitimate to think that the corresponding QS and ASCAT SLP_u10 winds should be in agreement as well. Indeed, we now show that, while there exist some discrepancies between ASCAT and QS winds, the statistical and spectral characteristics of ASCAT and QS/SLP_u10 winds are relatively similar. We therefore suggest that wind filtering via SLP retrieval might be a way to reconcile and harmonize current and future satellite wind data sets.

The wind statistics of Section III were repeated for both QS/SLP_u10 and AS/SLP_u10 winds. The results are shown as red and blue dashed lines in Figs. 2–7. Fig. 2 shows that the SLP_u10 wind speeds are smaller than the original wind speeds for both instruments. As noted by [12], the UWPBL filtering tends to reduce the wind speeds overall, although the effect is much smaller on ASCAT winds than on QS winds. The wind directions, however, are improved noticeably in the case of QS, while the filtering has little effect on the ASCAT winds, if not a negative effect. This confirms that the original ASCAT wind retrieval yields better directions than the QS wind retrieval. It also shows that the UWPBL filtering, which is efficient at correcting directional errors, but not wind speed errors, improves QS winds (i.e., increased R^2 when compared to buoys), but does not improve ASCAT winds, and possibly degrades them (i.e., decreased R^2, see Table I).

Fig. 5 shows that the speed standard deviation between QS/SLP_u10 and ECMWF winds is more homogeneous throughout the swath than it is for QS (i.e., the difference curve is more "flat"). It is due to the fact that a nadir wind vector is corrected based on the synoptic-scale structure of the UWPBL SLP field. Since the standard deviation in pressure between UWPBL SLP and ECMWF SLP is significantly reduced at nadir (see Fig. 10), the wind vectors newly derived from that smooth SLP field also have better characteristics, and the standard deviation in wind speed and direction is reduced as well.

In Fig. 5, the agreement between ASCAT and ECMWF, which is already better than for QS, is improved even more by filtering AS winds via the UWPBL SLP retrieval. Note again, however, that a better agreement with ECMWF 10-m wind analyses is not necessarily indicative of a higher accuracy. Since our earlier buoy comparisons showed that the SLP filtering does not improve the ASCAT wind directions (as compared to buoys), the better agreement with ECMWF suggests that the SLP-filtered ASCAT winds are not necessarily closer to the "truth," but only closer to ECMWF analyses, presumably because these are smoother and the SLP filtering removes some of the directional variability of the ASCAT winds. It is interesting to note, however, that the standard deviation of the wind direction differences between the ECMWF and *unfiltered* ASCAT surface winds is similar to the differences between ECMWF and the *filtered* QS surface winds. This is made even clearer in Fig. 6, where it can be seen that ASCAT and QS/SLP_u10 standard deviations are also similar in their seasonal variations, and that the similarities carry over to the speed standard deviations in the Northern Pacific and to some extent in the Southern Pacific Ocean as well. This suggests that filtering QS winds while leaving AS winds unchanged might be a way to align the two products, a point to which we will return later.

Finally, the similarities between ASCAT and QS/SLP_u10 winds are reinforced when considering their spectral characteristics in Fig. 7, where the SLP_u10 winds were obtained by only correcting the winds for directional errors (i.e., the wind speeds were kept unchanged). The QS/SLP_u10 spectrum follows a -2.4 power law down to the smallest scales (as determined by linear regression between 1600 and 100 km) and is very similar to the original ASCAT spectrum. Note that the *filtered* ASCAT spectrum shows signs of falling off, suggesting that the UWPBL filter might remove part of the geophysical information contained in the original signal, for reasons mentioned earlier (i.e., low-pass filtering associated with the least-squares minimization and smoothing of the UWPBL pressure fields). This reinforces the idea that the *unfiltered* ASCAT winds are quite similar to the *filtered* QS winds, as we now discuss.

VI. Discussion

Our results show that the SLP fields derived from ASCAT and QS winds using the UWPBL model share similar statistical characteristics. These SLP fields can be used to derive a new set of surface winds, which we expect to have improved characteristics, as compared to the original winds. We can view these new winds as *filtered* by the SLP retrieval, as the SLP fields effectively act as a filter on multiple scales, from the small to the synoptic scales. In particular, it is noteworthy that the filtered QS winds are in good agreement with the *un*filtered ASCAT winds. It is likely that the SLP filtering removes much of the small-scale noise present in QS winds due to the geometry of the antenna and rain contamination, while it does little to the ASCAT winds, which have a lower noise level. Therefore, since the methodology produces two wind data sets that are in better agreement in a statistical sense (based on three different comparative analyses), we propose that it might help align future scatterometer wind data sets and combine them into a single consistent record of the marine surface wind field.

Although it is beyond the scope of this study, it is also likely that mesoscale structures are captured effectively by the SLP retrieval and preserved when calculating a new set of surface winds by running the model in its direct mode. Indeed, Patoux *et al.* [35] have shown that QS winds contain mesoscale information about the genesis of frontal waves, while Patoux *et al.* in [26] have shown that they contain information about incipient midlatitude cyclones at the very first stage of their development. In each case, the mesoscale features are revealed in the vorticity of the winds filtered with the SLP retrieval methodology. We have verified visually on many cases that ASCAT winds also contain similar mesoscale information, although a rigorous comparison of the ability of the two instruments (QS and ASCAT, and in the near future, any other combination of ocean vector wind sensors) to capture the same information will require that we track the features of interest (e.g., fronts, frontal waves, incipient cyclones) and perform a quantitative comparison. This will be the subject of a future study and will constitute an additional basis for cross-calibrating and validating the two data sets.

A compelling argument for the filtering methodology can be seen in the spectral analysis of the wind vectors. The spectrum of the filtered QS winds follows a -2.4 power law down to 50 km. The slope of the unfiltered and filtered ASCAT wind spectra is -2.2 and -2.5, respectively. In an excellent review of energy cascades and the statistical structure of the atmospheric wind field, [36] note that many of the measured wind energy spectra published in the literature exhibit a power law behavior with slopes close to -2.4, which is the value predicted by isobaric turbulence (i.e., turbulence estimated from wind fluctuations following a pressure surface, rather than a horizontal surface). In that framework, the spectral behavior of vertical fluctuations of the horizontal wind, which has a slope of -2.4, is imparted to horizontal fluctuations down to a scale of about 40 km. Even though most of the wind measurements in past studies were performed by aircraft above the PBL, there is a possibility that scatterometer winds should reflect some of the same isobaric characteristics (Lovejoy, personal communication). For one thing, scatterometer wind model functions are derived from comparisons with NWP model analyses, which are essentially isobaric. Moreover, the PBL is characterized by strong vertical variations of the horizontal winds (i.e., Ekman turning, essentially), modulated by the combination of such processes as stratification, baroclinicity, secondary circulations, local accelerations, and ageostrophic frontal circulations. It is likely that such vertical variations impact horizontal fluctuations of the horizontal wind in ways that should be reflected in its spectral characteristics. To test this hypothesis, a future study will consist in isolating PBL regimes of interest and carrying out a comparative spectral analysis of the horizontal wind in both the horizontal and vertical direction. If valid, such an explanation would offer a compelling alternative to invoking an inverse cascade of small-scale energy along with a transition from 2-D to 3-D turbulence, particularly in view of recent results showing that most of the small-scale energy appearing in QS spectra might be due to noise [20]. A better understanding of the spectral characteristics of scatterometer wind measurements will be essential to understand the differences between various satellite wind data sets and reconcile them within a single data record of the marine surface wind field.

VII. Conclusion

We have shown that there exist statistical differences between ASCAT and QS winds. While QS winds are in better agreement with buoy measurements in terms of speed, ASCAT winds are in better agreement in terms of direction. ASCAT winds are also in better agreement with ECMWF analyses. In contrast, the SLP fields derived from ASCAT and QS winds using the UWPBL model are in very good agreement with each other, apart from a tendency for weaker ASCAT-derived pressure gradients when compared to buoys, which we ascribe to weaker winds in the ASCAT product, and some differences with ECMWF analyses in the tropics. Based on these results alone, we propose that the SLP retrieval might be a way of producing a continuous and consistent satellite-derived SLP record from multiple instruments, even if the original winds show some discrepancies.

We also propose that the swath-based SLP fields can be used to rederive a new set of wind vectors, which can then be used as a baseline for filtering the wind measurements from various instruments. The statistical characteristics of the different wind sets could be aligned by choosing the threshold directional difference above which the wind vectors should be changed, and by tuning the SLP retrieval appropriately, e.g., by smoothing the SLP fields with a low-pass filter before deriving the new wind vectors. In the present case, for example, it appears that QS and ASCAT wind directions could be made to agree by filtering QS wind directions while leaving ASCAT winds unchanged.

Currently, a shortcoming of the methodology is that the UWPBL model is not optimal in the tropics, and the "direct" methodology for deriving new wind vectors is not available, but the model is regularly undergoing improvements and, in the meantime, provides a baseline for orienting future research about the joint calibration and validation of satellite wind measurements by different instruments, and for producing a long-term record of both scatterometer-derived SLP fields and scatterometer winds.

Appendix
Slope of Pressure and Wind Spectra

By definition of the Fourier transform, if a process has a power spectrum $E(\omega)$, then the power spectrum of the derivative of that process is $\omega^2 E(\omega)$. If the spectrum of atmospheric surface pressure follows a power law of the form $E(\omega) = \omega^{\alpha}$, then the spectrum of the wind, which is essentially a derivative or pressure, should follow a power law of the form $\omega^2 E(\omega) = \omega^{\alpha+2}$. In the present analysis, the spectrum of the surface pressure fields derived from both QS and ASCAT measurements follows a power law of exponent $\alpha = -4.3$. Therefore, the SLP_u10 winds derived from those pressure fields should follow a power law of exponent $\alpha + 2 = -2.3$, which is close to the values of -2.4 and -2.5 obtained for QS and ASCAT, respectively.

ACKNOWLEDGMENT

The authors would like to thank Anton Verhoef for his help in obtaining ASCAT winds from OSI SAF, Don Percival for his continued interest in our research and valuable discussions about spectral analysis, as well as two anonymous reviewers for their insightful and constructive comments. The ds111.1 data were provided by ECMWF through the Data Support Section of the Computational and Information Systems Laboratory at NCAR.

REFERENCES

[1] R. F. Milliff, M. Freilich, W. Liu, R. Atlas, and W. Large, "Global ocean surface vector wind observations from space," in *Observing the Oceans in the 21st Century*, C. J. Koblinsky and N. R. Smith, Eds. Melbourne, Australia: GODAE Project Office Bureau Meteor., 2002, pp. 102–119.

[2] W. T. Liu, "Progress in scatterometer application," *J. Oceanogr.*, vol. 58, no. 1, pp. 121–136, Feb. 2002.

[3] A. Stoffelen, "Toward the true near-surface wind speed: Error modeling and calibration using triple collocation," *J. Geophys. Res.*, vol. 103, no. C4, pp. 7755–7766, 1998.

[4] A. Stoffelen, "A simple method for calibration of a scatterometer over the ocean," *J. Atmos. Ocean. Technol.*, vol. 16, no. 2, pp. 275–282, Feb. 1999.

[5] M. H. Freilich and R. S. Dunbar, "The accuracy of the NSCAT 1 vector winds: Comparisons with national data," *J. Geophys. Res.*, vol. 104, pp. 11 231–11 246, 1999.

[6] Y. Quilfen, B. Chapron, and D. Vandemark, "The ERS scatterometer wind measurement accuracy: Evidence of seasonal and regional biases," *J. Atmos. Ocean. Technol.*, vol. 18, no. 10, pp. 1684–1697, Oct. 2001.

[7] N. Ebuchi, "Evaluation of wind vectors observed by QuikSCAT/SeaWinds using ocean buoy data," *J. Atmos. Ocean. Technol.*, vol. 19, no. 12, pp. 2049–2062, Dec. 2002.

[8] M. G. Schlax, D. B. Chelton, and M. H. Freilich, "Sampling errors in wind fields constructed from single and tandem scatterometer datasets," *J. Atmos. Ocean. Technol.*, vol. 18, no. 6, pp. 1014–1036, Jun. 2001.

[9] M. Bourassa, D. Legler, J. O'Brien, and S. Smith, "SeaWinds validation with research vessels," *J. Geophys. Res.*, vol. 108, no. C2, pp. 1–16, 2003.

[10] D. B. Chelton and M. H. Freilich, "Scatterometer-based assessment of 10-m wind analyses from the operational ECMWF and NCEP numerical weather prediction models," *Mon. Wea. Rev.*, vol. 133, no. 2, pp. 409–429, Feb. 2005.

[11] J. Patoux, R. C. Foster, and R. A. Brown, "An evaluation of scatterometer-derived oceanic surface pressure fields," *J. Appl. Meteor. Climatol.*, vol. 47, no. 3, pp. 835–852, Mar. 2008.

[12] J. Patoux, R. C. Foster, and R. A. Brown, "A method for including mesoscale and synoptic-scale information in scatterometer wind retrievals," *J. Geophys. Res.*, vol. 115, p. D11 105, 2010.

[13] J. N. Huddleston and B. W. Stiles, "A multidimensional histogram rain-flagging technique for seawinds on QuikSCAT," in *Proc. IEEE Geosci. Remote Sens. Symp.*, Honolulu, HI, 2000, pp. 1232–1234.

[14] B. W. Stiles, *Special Wind Vector Data Product: Direction Interval Retrieval With Thresholded Nudging (DIRTH)*. Pasadena, CA: JPL, 1999.

[15] C. W. Fairall, E. F. Bradley, J. E. Hare, A. A. Grachev, and J. B. Edson, "Bulk parameterization of air-sea fluxes: Updates and verification for the COARE algorithm," *J. Clim.*, vol. 16, no. 4, pp. 571–591, Feb. 2003.

[16] X. Yuan, J. Patoux, and C. Li, "Satellite-based midlatitude cyclone statistics over the Southern Ocean. Part II: Tracks and surface fluxes," *J. Geophys. Res.*, vol. 114, no. D4, p. D04 106, 2009.

[17] B. Stiles, B. Pollard, and R. Dunbar, "Direction interval retrieval with thresholded nudging: A method for improving the accuracy of QuikSCAT winds," *IEEE Trans. Geosci. Remote Sens.*, vol. 40, no. 1, pp. 79–89, Jan. 2002.

[18] M. H. Freilich and D. B. Chelton, "Wavenumber spectra of Pacific winds measured by the Seasat scatterometer," *J. Phys. Oceanogr.*, vol. 16, no. 4, pp. 741–757, Apr. 1986.

[19] J. Patoux and R. A. Brown, "Spectral analysis of QuikSCAT surface winds and two-dimensional turbulence," *J. Geophys. Res.*, vol. 106, no. D20, pp. 23 995–24 005, 2001.

[20] E. Rodríguez and A. Chau, "Improved wind directions, divergence, vorticity and their spectra for the QuikSCAT scatterometer," *J. Geophys. Res.*, 2011, submitted for publication.

[21] D. B. Chelton, M. H. Freilich, J. M. Sienkiewicz, and J. Von Ahn, "On the use of QuikSCAT scatterometer measurements of surface winds for marine weather prediction," *Mon. Wea. Rev.*, vol. 134, no. 8, pp. 2055–2071, Aug. 2006.

[22] R. F. Milliff, J. Morzel, D. B. Chelton, and M. H. Freilich, "Wind stress curl and wind stress divergence biases from rain effects on QSCAT surface wind retrievals," *J. Atmos. Ocean. Technol.*, vol. 21, no. 8, pp. 1216–1231, Aug. 2004.

[23] R. F. Milliff, W. G. Large, J. Morzel, and G. Danabasoglu, "Ocean general circulation model sensitivity to forcing from scatterometer winds," *J. Geophys. Res.*, vol. 104, no. C5, pp. 11 337–11 358, 1999.

[24] C. K. Wikle, R. F. Milliff, and W. G. Large, "Surface wind variability on spatial scales from 1 to 1000 km observed during TOGA COARE," *J. Atmos. Sci.*, vol. 56, no. 13, pp. 2222–2231, Jul. 1999.

[25] T. M. Chin, R. F. Milliff, and W. G. Large, "Basin-scale, high-wavenumber sea surface wind fields from a multiresolution analysis of scatterometer data," *J. Atmos. Ocean. Technol.*, vol. 15, no. 3, pp. 741–763, Jun. 1998.

[26] J. Patoux, X. Yuan, and C. Li, "Satellite-based midlatitude cyclone statistics over the Southern Ocean. Part I: Scatterometer-derived pressure fields and storm tracking," *J. Geophys. Res.*, vol. 114, no. D4, p. D04 105, 2009.

[27] R. A. Brown, "On two-layer models and the similarity functions for the planetary boundary layer," *Bound.-Layer Meteor.*, vol. 24, no. 4, pp. 451–463, Dec. 1982.

[28] R. A. Brown and G. Levy, "Ocean surface pressure fields from satellite sensed winds," *Mon. Wea. Rev.*, vol. 114, no. 11, pp. 2197–2206, Nov. 1986.

[29] J. Patoux, R. C. Foster, and R. A. Brown, "Global pressure fields from scatterometer winds," *J. Appl. Meteor.*, vol. 42, no. 6, pp. 813–826, Jun. 2003.

[30] J. Patoux and R. A. Brown, "A gradient wind correction for surface pressure fields retrieved from scatterometer winds," *J. Appl. Meteor.*, vol. 41, no. 1, pp. 133–143, 2002.

[31] R. A. Brown and L. Zeng, "Estimating central pressures of oceanic midlatitude cyclones," *J. Appl. Meteor.*, vol. 33, no. 9, pp. 1088–1095, 1994.

[32] J. Patoux and R. A. Brown, "A scheme for improving scatterometer surface wind fields," *J. Geophys. Res.*, vol. 106, no. D20, pp. 23 985–23 994, 2001.

[33] D. B. Chelton, M. H. Freilich, and S. Esbensen, "Satellite observations of the wind jets off the Pacific coast of Central America. Part I: Case studies and statistical characteristics," *Mon. Wea. Rev.*, vol. 128, no. 7, pp. 1993–2018, Jul. 2000.

[34] D. B. Chelton, "The impact of SST specification on ECMWF surface wind stress fields in the Eastern Tropical Pacific," *J. Clim.*, vol. 18, no. 4, pp. 530–550, Feb. 2005.

[35] J. Patoux, G. J. Hakim, and R. A. Brown, "Diagnosis of frontal instabilities over the Southern Ocean," *Mon. Wea. Rev.*, vol. 133, no. 4, pp. 863–875, Apr. 2005.

[36] S. Lovejoy and D. Schertzer, "Towards a new synthesis for atmospheric dynamics: Space-time cascades," *Atmos. Res.*, vol. 96, no. 1, pp. 1–52, Apr. 2010.

Jérôme Patoux received the Ph.D. degree in atmospheric sciences from the University of Washington, Seattle, in 2003.

He is currently a Research Assistant Professor with the Department of Atmospheric Sciences, University of Washington. He is a member of the NASA International Ocean Vector Winds Science Team.

Ralph C. Foster received the Ph.D. degree in atmospheric sciences from the University of Washington, Seattle, in 1996.

He is currently a Physicist with the Applied Physics Laboratory, University of Washington. He is a member of the NASA International Ocean Vector Winds Science Team.